PNAS RESEARCH ARTICLE | APPLIED BIOLOGICAL SCIENCES OPEN ACCESS

The red alga *Porphyridium* as a host for molecular farming: Efficient production of immunologically active hepatitis C virus glycoprotein

Alexander Hammel[a,1], Lia-Maria Cucos[b,1], Iuliana Caras[c], Irina Ionescu[c], Catalin Tucureanu[c], Vlad Tofan[c], Adriana Costache[c], Adrian Onu[c], Lara Hoepfner[d], Michael Hippler[d,e], Juliane Neupert[a], Costin-Ioan Popescu[b], Crina Stavaru[c,2], Norica Branza-Nichita[b,2], and Ralph Bock[a,f,2]

Contributed by Ralph Bock; received January 8, 2024; accepted May 3, 2024; reviewed by Kyle Lauersen and Alexander W. Tarr

Microalgae are promising production platforms for the cost-effective production of recombinant proteins. We have recently established that the red alga *Porphyridium purpureum* provides superior transgene expression properties, due to the episomal maintenance of transformation vectors as multicopy plasmids in the nucleus. Here, we have explored the potential of *Porphyridium* to synthesize complex pharmaceutical proteins to high levels. Testing expression constructs for a candidate subunit vaccine against the hepatitis C virus (HCV), we show that the soluble HCV E2 glycoprotein can be produced in transgenic algal cultures to high levels. The antigen undergoes faithful posttranslational modification by N-glycosylation and is recognized by conformationally selective antibodies, suggesting that it adopts a proper antigenic conformation in the endoplasmic reticulum of red algal cells. We also report the experimental determination of the structure of the N-glycan moiety that is attached to glycosylated proteins in *Porphyridium*. Finally, we demonstrate the immunogenicity of the HCV antigen produced in red algae when administered by injection as pure protein or by feeding of algal biomass.

molecular farming | red alga | vaccine | biopharmaceutical | hepatitis

Significance

Algae represent promising production factories for the large-scale synthesis of recombinant proteins in photosynthetic organisms, also referred to as molecular farming. However, only relatively few algal species are currently amenable to genetic engineering, and the high-level production of foreign proteins remains challenging. Here, we have explored the potential of a red alga to synthesize a candidate vaccine against the hepatitis C virus (HCV) that is causally responsible for more than 58 million chronic infections worldwide. We show that high levels of functional HCV E2 glycoprotein can be produced in the red alga *Porphyridium purpureum*. Importantly, the protein elicits an HCV-specific immune response when injected into experimental animals, and also supports a primed immune response upon feeding of algal biomass.

Microalgae are promising new production platforms for therapeutic proteins. They combine the attraction of photoautotrophic growth with the possibility to utilize bioreactor-based microbial cultivation techniques, and the capability to perform complex posttranslational modifications (1). Further advantages include inexpensive scalability, no competition for agricultural land, and minimal safety concerns (2, 3).

Unfortunately, progress in microalgal biotechnology has been hindered by the lack of molecular tools for high-level expression of recombinant proteins in suitable algal species. The most advanced toolbox in microalgal biology is available for the model organism *Chlamydomonas reinhardtii*, making it by far the most utilized microalga for biotechnological applications (4–7). However, high-level nuclear transgene expression remains challenging, and often, the attainable recombinant protein levels are too low to be competitive with established microbial production systems (8–16).

We recently reported that the red microalga *Porphyridium purpureum* displays a number of favorable properties for recombinant protein production. Transformed microalgal cells maintain the transformation vector episomally at a high copy number, leading to high transgene accumulation levels (17). *P. purpureum* can accumulate recombinant proteins to levels of up to 5% of the total soluble protein and possesses the ability to effectively secrete proteins into the culture medium (18). To assess whether the red alga provides a competitive production platform for the synthesis of high-value recombinant proteins, here we have investigated the expression of a modified version of the E2 surface glycoprotein of the hepatitis C virus (HCV), a promising subunit vaccine candidate.

Infection with HCV currently affects more than 58 million people worldwide. 1.5 million new cases are reported each year, making this pathogen a significant health problem (19). Although the standard of care has substantially improved by the approval of efficient antivirals, diagnosis, and treatment accessibility remain low at the global level (20). Moreover, HCV-cured patients are susceptible to reinfection. Thus, the ambitious WHO goal to eliminate HCV infection as a public health problem by 2030 is unlikely to be met in the absence of prevention of infections by vaccination (21).

As an RNA virus, HCV exhibits high genetic diversity, making the development of a vaccine capable of inducing an efficient humoral immune response against neutralization-resistant strains extremely challenging (22). The E2 envelope glycoprotein enables HCV internalization through interactions with the host cell receptors SR-BI and CD81 expressed

Reviewers: K.L., King Abdullah University of Science and Technology; and A.W.T., The University of Nottingham.

The authors declare no competing interest.

[1]A.H. and L.-M.C. contributed equally to this work.

[2]To whom correspondence may be addressed. Email: stavaru34@yahoo.com, nichita@biochim.ro, or rbock@mpimp-golm.mpg.de.

This article contains supporting information online at https://www.pnas.org/lookup/suppl/doi:10.1073/pnas.2400145121/-/DCSupplemental.

Published June 4, 2024.

on hepatocytes, and therefore, is the main target of virus-neutralizing antibodies (23). HCV E2 forms a heterodimer with the E1 envelope glycoprotein believed to enable the fusion step in the entry process (24–26). As main vaccine candidates targeting the humoral immune response, E1 and E2 have been produced in various expression hosts for structural and immunological studies, and the E1E2 heterodimer expressed in CHO cells was used in initial clinical trials (27). In addition to therapeutic immunization in patients with chronic HCV, phase I clinical trials of E1E2 vaccines have been performed in healthy human volunteers (28). Different E2 variants lacking the transmembrane domain were expressed in mammalian and insect cells to investigate antigen conformation and immunological properties (29–33). In an effort to produce a candidate vaccine at low cost, we recently expressed the E2 protein in plants, both alone and as E1E2 transmembrane heterodimer, and demonstrated the ability of the antigens to induce a virus-neutralizing humoral immune response (34, 35).

The N terminus of the E2 protein spans the hypervariable region 1 (HVR1) and is characterized by a high intra- and intergenotype variability. The HVR1 domain has the ability to activate B cell clonotypes of reduced neutralization capacity (33). Thus, removing this region has emerged as a vaccine design to potentially induce broadly neutralizing anti-HCV antibodies. Additional deletion of the transmembrane domain enables protein secretion, facilitating downstream purification steps. The resulting antigen is a soluble protein containing 11 N-linked glycans and 9 disulfide bridges, which follows a similar folding pathway and exhibits similar stability as the wild-type HCV E2 (33, 36–38).

In this work, we expressed in premiere a vaccine candidate in *P. purpureum,* the soluble HCV E2 glycoprotein lacking the HVR1 ($sE2^{\Delta HVR1}$). We report the high-level production of a functional, N-glycosylated HCV antigen, indicating the presence of an appropriate folding milieu within the endoplasmic reticulum (ER) of the red alga. Furthermore, we determined an N-glycan moiety that is attached to a glycoprotein expressed in *P. purpureum*. Finally, we demonstrate that the produced HCV antigen elicits a humoral immune response in mice upon injection, and supports a primed immune response upon feeding of algal biomass.

Results

HCV Antigen Design and Expression in *P. purpureum* and *C. reinhardtii*. To comparatively assess the expression of the $E2^{\Delta HVR1}$ antigen in green versus red algal cells, transformation vectors for *P. purpureum* and *C. reinhardtii* were constructed for the expression of antigen variants targeted to different subcellular destinations (Fig. 1). $E2^{\Delta HVR1}$ is an antigen whose native (antigenic) conformation is dependent on the acquisition of posttranslational modifications (PTMs) in the ER. To test different protein localizations and assess the efficacy of ER translocation, we constructed three antigen variants for accumulation in the cytosol ($*E2^{\Delta HVR1}$), secretion ($sE2^{\Delta HVR1}$), or ER retention ($E2^{\Delta HVR1\text{-}HDEL}$). To confer translocation into the ER, the signal peptide of carbonic anhydrase 1 was incorporated at the N terminus. An ER retention signal (HDEL) was incorporated C-terminally to allow protein accumulation in the ER and prevent potential modification along the secretory pathway. All variants contained a 3xHA tag to facilitate antigen detection. In *P. purpureum,* the expression of all three variants is controlled by the endogenous actin promoter and terminator, whereas the genes for expression in *C. reinhardtii* are driven by the strong *PsaD* promoter and terminator (Fig. 1*A*). Our construct design does not include introns, a common practice for transgene expression in *C. reinhardtii* (39). Instead, expression in the green alga was facilitated by the use of the expression strain UVM11 (4, 7). In *P. purpureum*, an additional construct containing the $sE2^{\Delta HVR1}$ antigen driven by the endogenous chlorophyll a binding protein (*ChlBP*) promoter, recently shown to facilitate high-level YFP accumulation, was also tested (Fig. 2*D*; 18). Finally, a His-tagged version of the antigen targeted for secretion was constructed for expression in the red alga to enable purification and parenteral administration, by exchanging the 3xHA tag with a 6xHis tag (*SI Appendix*, Fig. S2).

For each construct, several transgenic algal clones were isolated, and their antigen accumulation levels were determined by semi-quantitative immunoblotting using a 3xHA-tagged YFP as a standard. Antigen accumulation was detected for all variants transformed into *P. purpureum*, at levels reaching up to 0.5% of the total protein (TP). By contrast, *C. reinhardtii* transformants exhibited significantly lower levels of recombinant protein production, with the best-performing strains accumulating the antigen to 0.14% of TP (Fig. 1*B*) The superior expression properties of *P. purpureum* are in line with a previous study that had compared YFP expression in the two algal species (18). The mass shift visible in the $sE2^{\Delta HVR1}$ and $E2^{\Delta HVR1\text{-}HDEL}$ variants compared to the cytosolic version indicates successful ER translocation and glycosylation of the antigen. Interestingly, the glycosylation patterns seem to differ between *C. reinhardtii* and *P. purpureum,* as evidenced by the different sizes of the antigens targeted for secretion and ER retention. This finding is in agreement with a recent bioinformatic analysis that predicted protein glycosylation patterns in microalgae (40).

P. purpureum maintains the transformation vector episomally at a high copy number per cell (17). Consequently, expression levels should be unaffected by position effects, in contrast to *C. reinhardtii*, where transgenes integrate into random locations within the genome. The variation between the two lines expressing the antigen targeted for secretion ($sE2^{\Delta HVR1}$) and the ER-retained antigen ($sE2^{\Delta HVR1\text{-}HDEL}$) is likely explained by contamination of the primary transformed algal colonies with residual wild-type cells, which represents a common phenomenon in *Porphyridium* transformation (Figs. 1*B* and 2; 18). This heterogeneity can be eliminated by purifying the transgenic strain via further rounds of colony formation from single cells (Fig. 2*A*).

Secretion of the antigen could not be detected in primary transformed lines, but was later demonstrated for lines expressing the *ChlBP* promoter-driven $sE2^{\Delta HVR1}$ antigen (Fig. 2*D*). The initial failure to detect the protein in the medium was most likely due to low secretion efficiency and/or proteolytic degradation of the antigen in the medium. The strains expressing the antigen from the *ChlBP* promoter showed increased accumulation of the antigen in the culture medium, as compared to transgenic strains expressing the identical protein from the actin promoter, indicating higher expression of the secretion-competent viral protein.

Because *P. purpureum* showed superior expression compared to *C. reinhardtii*, the red microalga was used for all further experiments.

HCV E2 Antigens Expressed in *P. purpureum* and Mammalian Cells Have Similar N-Glycosylation Patterns. To determine whether the HCV antigens are N-glycosylated in *P. purpureum,* cells expressing $sE2^{\Delta HVR1}$ (Fig. 1 *C* and *D*) or $E2^{\Delta HVR1\text{-}HDEL}$ (Fig. 1*D*) were incubated for various times with increasing concentrations of tunicamycin (TM), a potent inhibitor of protein N-glycosylation (41). TM treatment resulted in a significant decrease of the apparent molecular weight of the antigens by about 20 kDa, accounting for the loss of E2 N-linked glycans as revealed by immunoblotting. Interestingly, a minute amount of nonglycosylated polypeptide was detectable in the absence of TM treatment in the $sE2^{\Delta HVR1}$ but not

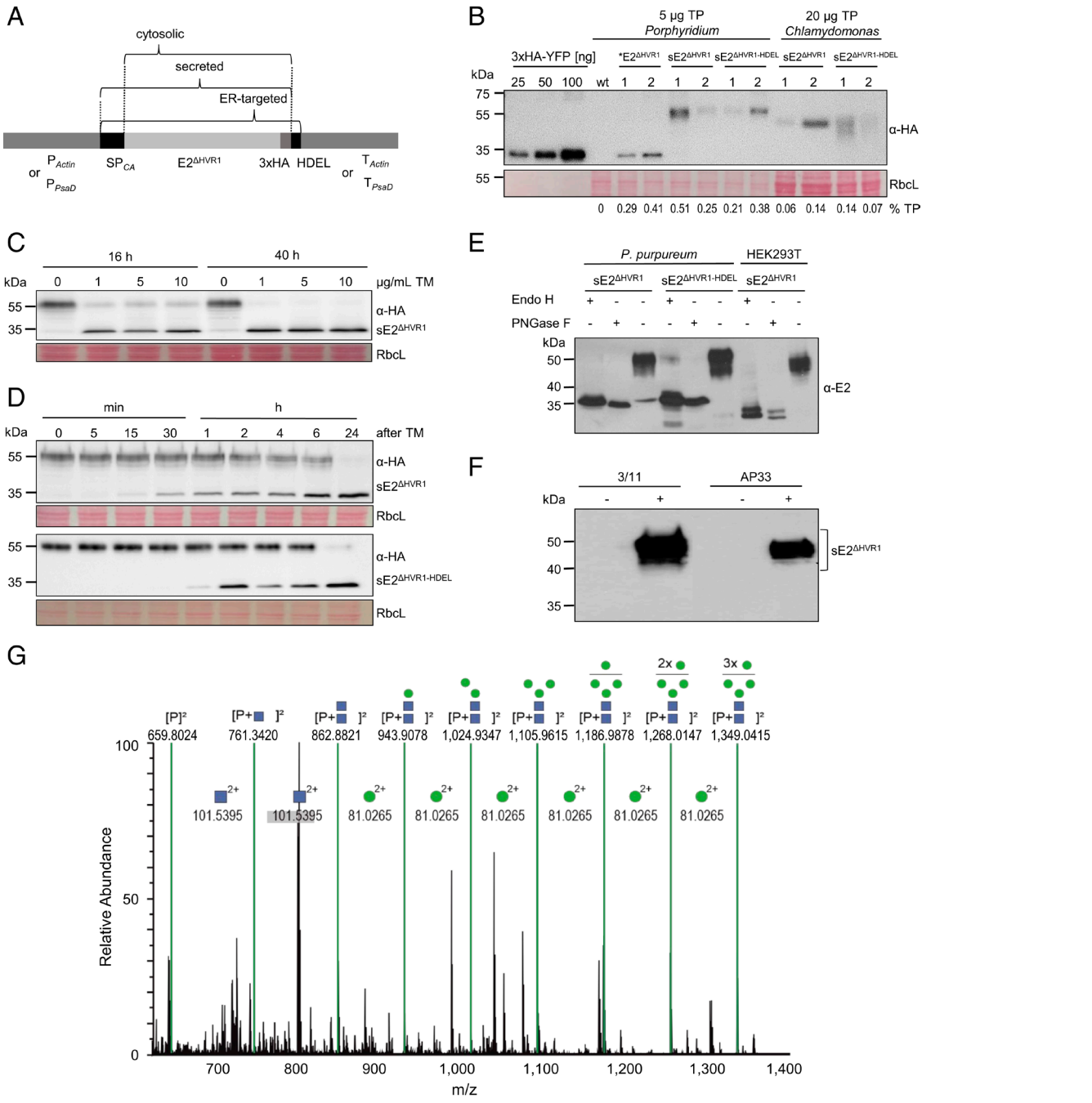

Fig. 1. Expression of HCV antigens and analysis of N-glycosylation. (*A*) Schematic representation of the E2$^{\Delta HVR1}$ constructs. A cytosolic (*E2$^{\Delta HVR1}$), a secreted (sE2$^{\Delta HVR1}$), and an ER-targeted (sE2$^{\Delta HVR1\text{-}HDEL}$) version were designed. The signal peptide of the carbonic anhydrase from the red alga and the green alga, respectively, was incorporated upstream of the codon-optimized antigen-coding sequence for the secreted and ER-targeted antigen versions. A C-terminal HDEL motif was additionally incorporated in the ER-targeted antigen. All antigens carry a 3xHA-tag for detection by immunoblotting. For expression in *P. purpureum*, the promoter (and 5′UTR) and terminator of the actin gene were used. For expression in *C. reinhardtii*, the *PsaD* promoter and terminator were used. (*B*) Immunoblot analysis of E2$^{\Delta HVR1}$-expressing *P. purpureum* and *C. reinhardtii* strains. Samples of 5 µg total protein of two independently generated transgenic *P. purpureum* lines each (1 and 2) expressing the three differently localized variants of E2$^{\Delta HVR1}$ and 20 µg of total protein of *C. reinhardtii* lines (1 and 2) expressing the secreted or the ER-retained variants of E2$^{\Delta HVR1}$ were analyzed. Antigen signals were detected with an HA-specific antibody. The region of the Ponceau-stained membrane containing the large subunit of Rubisco (RbcL) clearly shows the difference in loading between the two algae. A dilution series of recombinant 3xHA-YFP was used as standard for semiquantitative assessment of expression levels. Estimated accumulation levels of the antigen are shown below each lane (in percent of the total protein; TP). (*C*) Test of the glycosylation inhibitor tunicamycin (TM) on *P. purpureum* cells expressing the sE2$^{\Delta HVR1}$ antigen. Samples of cells grown in medium with different TM concentrations were taken after 16 h and 40 h. Samples of 20 µg total protein were separated by SDS-PAGE (12% gel) and analyzed by immunoblotting with an anti-HA antibody. Equal loading was verified by Ponceau staining of the membrane, and the region containing RbcL is shown below the blot. (*D*) 1 µg/mL TM was added to cultures with a density of 4.5 × 10^6 cells/mL of transgenic strains expressing sE2$^{\Delta HVR1}$ or E2$^{\Delta HVR1\text{-}HDEL}$. The cultures were grown for 24 h and samples for immunoblot analysis were taken at the indicated time points. Samples of 20 µg total protein were separated by SDS-PAGE (12% gel) and analyzed by immunoblotting with an HA-specific antibody. Equal loading was confirmed by Ponceau staining, with the region containing RbcL being shown below the blot. (*E*) Soluble protein extracts from HEK293T cells and *P. purpureum* cell lysates expressing E2$^{\Delta HVR1}$ either as a secreted protein or retained in the ER by a HDEL sequence motif were subjected to Endo H or PNGase F digestion (+) or left untreated (−), then separated by SDS-PAGE (10% gel) and analyzed by immunoblotting. Glycosylated and deglycosylated polypeptides were detected using anti-E2 H47 antibodies. (*F*) sE2$^{\Delta HVR1}$ recognition in *P. purpureum* lysates (+) by immunoblot analysis using anti-E2 3/11 or AP33 as primary antibodies. Wild-type *P. purpureum* (−) was loaded as a negative control for antibody specificity. (*G*) Mass spectrometric analysis of the HCV peptide HKFNSSGCPER. The averaged MS1 spectrum of doubly charged, N-glycosylated peptide ions (P) differing in glycan composition and chain length is shown. The MS2 spectrum, confirming the identity of the peptide, is shown in *SI Appendix*, Fig. S3. Blue squares: HexNac; green circles: Hex.

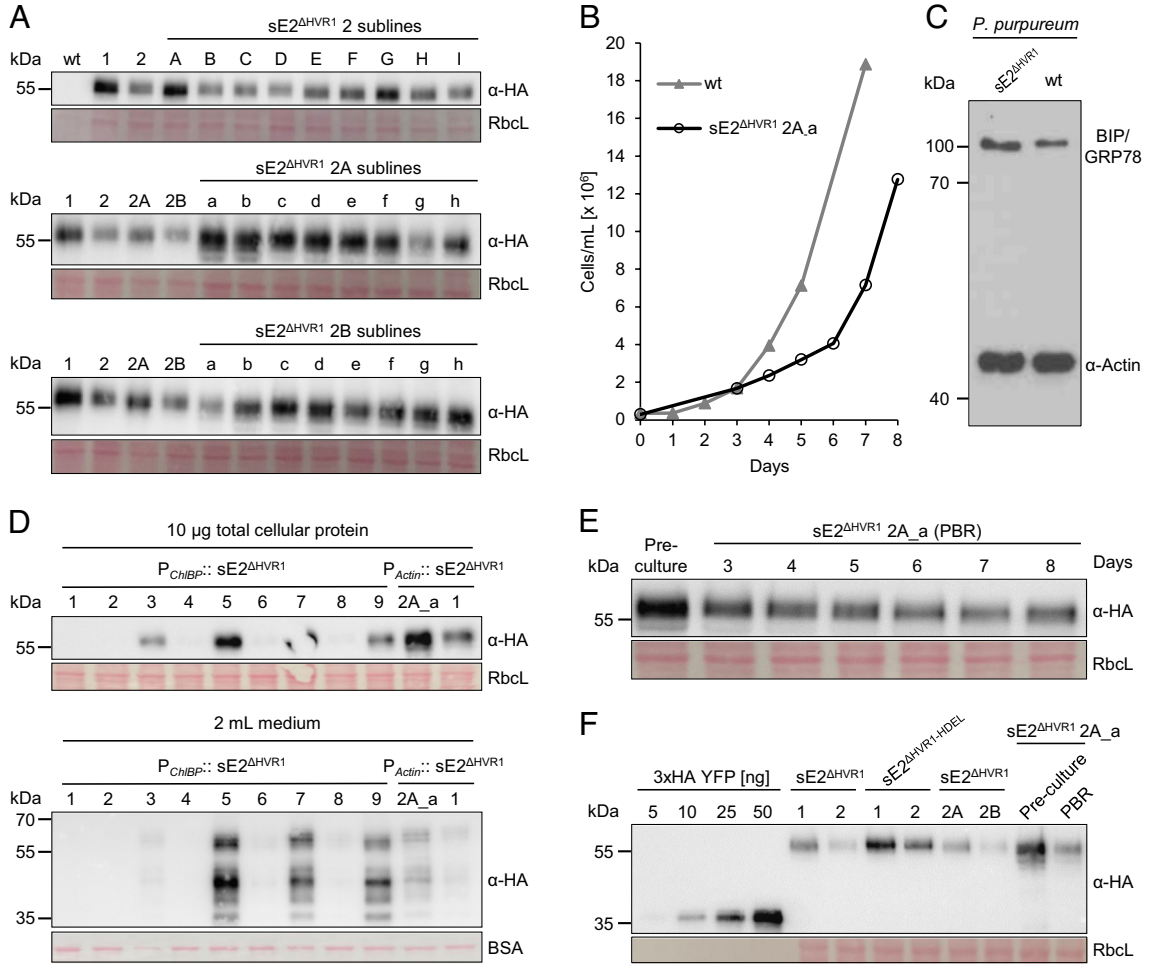

Fig. 2. Generation, purification, and characterization of *P. purpureum* strains expressing sE2$^{\Delta HVR1}$. (*A*) Single colonies of sE2$^{\Delta HVR1}$ line 2 were generated using the starch plating method (*Materials and Methods*), and nine colonies (A-I) were picked and analyzed by immunoblotting. Samples of 5 µg total protein of sE2$^{\Delta HVR1}$-expressing lines 1 and 2 were loaded next to 5 µg total protein of the sublines derived from sE2$^{\Delta HVR1}$ line 2 (*Upper*). Out of these sublines, a high (2A) and a medium (2B) expressing line were selected; single cell lines were generated again and analyzed by immunoblotting (*Middle and Bottom*). Ponceau staining of the membrane (with the RbcL region shown below each blot) served as loading control. (*B*) Example growth curve of wild-type cells and the sE2$^{\Delta HVR1}$ 2A_a strain grown in a photobioreactor. The initial cell number was adjusted to 3 × 10^5 cells/mL. (*C*) BiP expression in *P. purpureum* lysates as detected by immunoblot analysis using actin as loading control. (*D*) Immunoblot analysis of *P. purpureum* lines expressing sE2$^{\Delta HVR1}$ under the control of the strong endogenous *ChlBP* promoter. Samples of 10 µg total cellular protein extracted from nine independent zeocin-resistant lines were analyzed by immunoblotting using an anti-HA antibody, and compared to the lines sE2$^{\Delta HVR1}$ 2A_a and sE2$^{\Delta HVR1}$ 1, in which antigen expression is under transcriptional control of the actin gene promoter. Ponceau staining was used as loading control and the region containing RbcL is shown below the blot. Protein from the culture medium was also collected, and the equivalent of 2 mL medium was analyzed by immunoblotting. Spiked-in BSA can be seen in the Ponceau staining of the medium samples. (*E*) Immunoblot analysis of sE2$^{\Delta HVR1}$ antigen accumulation throughout the cultivation in the PBR. Ten microgram of total protein obtained from the preculture was loaded along with 10 µg of total protein sampled from the bioreactor at the indicated days after inoculation. (*F*) Quantification of different sE2$^{\Delta HVR1}$ variants using a 3xHA-tagged YFP standard. Ten microgram of total protein obtained from cultures grown either in the bioreactor (PBR) or in flasks (all other samples) were analyzed using the anti-HA antibody. The HCV antigen in the PBR accumulates to approximately 0.21% of TP.

the E2$^{\Delta HVR1\text{-}HDEL}$ sample, suggesting that prolonged ER retention may enhance the efficiency of N-glycosylation in *P. purpureum*.

To compare the glycosylation patterns of the antigens expressed in algae and mammalian cells, we performed digestions with endoglycosidases followed by immunoblotting and detection with nonconformational anti-E2 H47 antibodies (Fig. 1*E*). Control samples not treated with glycosidases showed a heterogeneous band of ~45 to 50 kDa in mammalian cells, which corresponds to the predicted molecular weight of the fully glycosylated sE2$^{\Delta HVR1}$ (29). The slightly lower electrophoretic mobility of the *P. purpureum* samples reflects the presence of the 3xHA sequence (adding ~3 kDa) fused to the C terminus of the sE2$^{\Delta HVR1}$ antigen. Treatment of cell lysates with PNGase F, an amidase that cleaves high-mannose, hybrid, and complex N-glycans from the asparagine residues of glycoproteins, generated sharp bands corresponding to the deglycosylated proteins (Fig. 1*E*). Efficient PNGase F cleavage tentatively indicated absence of core α-1,3-fucose glycans (that are common in seed plants), as this type of glycan moiety prevents deglycosylation by PNGase F. This preliminary conclusion was later confirmed by mass spectrometry (see below).

Notably, two protein species were detected after PNGase F digestion of the mammalian cell–derived sE2$^{\Delta HVR1}$ antigen. The upper band of the doublet likely represents the fraction of E2 polypeptides that also contain O-linked oligosaccharides, as previously documented (42). These modified proteins seem to be absent from *P. purpureum*. Sample treatment with Endo H, which cleaves the covalent bond between the first two N-acetylglucosamine residues of high-mannose N-linked glycans produced a similar pattern as treatment with PNGase F. Complete sensitivity of the sE2$^{\Delta HVR1}$ antigen to Endo H indicates the presence of high-mannose oligosaccharides, characteristic of E2 expressed in mammalian cells (43), and suggests conservation of this N-glycosylation pattern in *P. purpureum*. As observed before (Fig. 1 *C* and *D*), a small proportion of the sE2$^{\Delta HVR1}$ remains nonglycosylated in *P. purpureum*,

as revealed by the band with an electrophoretic mobility similar to that of the deglycosylated polypeptide in the presence of PNGase F (Fig. 1*E*). This behavior is suggestive of a rapid egress of sE2$^{\Delta HVR1}$ out of the ER in the absence of an ER-retention signal, as expected for the E2 protein lacking the transmembrane domain (44). To rule out potential nonspecific reactivity of E2 antibodies with endogenous algal proteins, lysates of wild-type *P. purpureum* were also probed with anti-E2 antibodies (Fig. 1*F*).

The HCV antigen was also detected in the culture medium, albeit the protein was partially degraded (Fig. 2*D*). The observed instability of the secreted antigen is likely due to activity of extracellular proteases that are secreted by *P. purpureum* cells into the medium (18). Circumstantial evidence for this explanation was provided by culture experiments in the presence of protease inhibitors, which resulted in improved protein stability in the medium (*SI Appendix*, Fig. S1).

Trafficking of the sE2$^{\Delta HVR1}$ beyond the ER enables advanced N-glycan processing with potential impact on the immunogenic properties of the antigen. We, therefore, selected this antigen for further characterization and immunological studies. As recovery of large amounts of protein from the culture medium will require additional optimization, we focused on the efficiently expressed intracellular protein.

***P. purpureum*–Derived sE2$^{\Delta HVR1}$ Antigen Contains Short-Chain, High-Mannose N-Linked Sugars.** Very little is known about protein glycosylation in red algae. To determine the structure of the N-glycan chains of the HCV antigen protein expressed in *P. purpureum*, we performed in-source-MS/MS. The analysis confirmed N-glycosylation of HCV peptide HKFNSSGCPER (*SI Appendix*, Fig. S3), an internal tryptic peptide that had been shown previously to be readily detectable by MS-based proteomics (45). The IS-CID-MS1 spectrum (Fig. 1*G*) showed signals of the peptide modified by two HexNAc and a minimum of six hexose residues, classifying the glycan as oligomannosidic (*SI Appendix*, Table S1). No peaks indicative of glycan modification by pentose, deoxyhexose residues, or methylation of hexose residues could be identified. Further HCD-fragmentation of m/z 761.3420 corresponding to m/z of [peptide + HexNac]2 allowed determination of the peptide sequence and identification of the glycosylation site based on the main sequence ions (annotated in Fig. 1*G*).

These data demonstrate that the sE2$^{\Delta HVR1}$ antigen expressed in red algal cells undergoes posttranslational modification by attachment of short-chain, high-mannose N-linked sugars, and are in agreement with the full sensitivity to Endo H digestion (Fig. 1*E*).

Purification of Transgenic *P. purpureum* Lines Expressing sE2$^{\Delta HVR1}$ and Biomass Production in a Photobioreactor (PBR). As mentioned above, variation between transgenic red algal strains expressing the same construct (sE2$^{\Delta HVR1}$ lines 1 and 2) usually comes from unwanted cocultivation with wild-type cells that survived in the shade of zeocin-resistant transformed cells. To eliminate this variation and purify the transgenic strains to homogeneity, single colonies were isolated from the strain showing lower expression (sE2$^{\Delta HVR1}$ line 2). Nine subclones were picked, cultured, and analyzed by immunoblotting (Fig. 2*A*). The subclones sE2$^{\Delta HVR1}$ 2A to I showed varying antigen accumulation ranging from high levels (comparable to sE2$^{\Delta HVR1}$ 1) in subclones A and G to low levels in subclone D. In a second purification round, single colony–derived subclones of sE2$^{\Delta HVR1}$ 2A (high level of antigen accumulation) and of sE2$^{\Delta HVR1}$ 2B (medium level of antigen accumulation) were generated, and antigen levels were again analyzed by immunoblotting. All subclones of sE2$^{\Delta HVR1}$ 2A showed high antigen accumulation (that even surpassed accumulation levels in sE2$^{\Delta HVR1}$ 1), tentatively suggesting that this strain was now homogeneously transgenic.

Strains sE2$^{\Delta HVR1}$ 2A_a and sE2$^{\Delta HVR1}$-6xHis line 5 were chosen for growth in a PBR to generate sufficient amounts of biomass for immunization experiments. Algal biomass from the strain expressing high levels of the 3xHA-tagged sE2$^{\Delta HVR1}$ became available first and was used for direct feeding of mice (oral immunization). The strain expressing the 6xHis-tagged antigen was used for antigen purification and injection-based immunization in a second, independent animal trial performed subsequently. Transgenic sE2$^{\Delta HVR1}$ 2A_a cells were grown for 8 d, until a sufficiently high cell density had been reached. In parallel, the *P. purpureum* wild-type strain was grown under the same conditions to serve as control in the feeding experiments. The sE2$^{\Delta HVR1}$-6xHis-expressing algal strain was grown in a different batch.

Notably, a slower growth rate was observed for the *P. purpureum* strain expressing the sE2$^{\Delta HVR1}$ antigen (38.3 h doubling time), compared to the wild-type control (27.6 h doubling time; Fig. 2*B*). To determine whether this growth delay was due to cellular stress induced by constitutive synthesis of high levels of the HCV protein, expression of BiP, a molecular chaperone and key regulator of unfolded protein response (UPR) signaling in the ER, was investigated in the cell lysates (46). The UPR is conserved in mammalian and plant cells and, recently, was also reported in *C. reinhardtii* (47). Although some canonical UPR signaling components are missing from unicellular green algae, BiP is highly expressed and plays similar roles in protein homeostasis as in higher eukaryotes (48, 49). To analyze BiP conservation in *P. purpureum*, we used the inferred protein sequence (A0A5J4Z1M8) from Uniprot and blasted it against the known sequence of human BiP (P11021) using Clustal Omega (EMBL-EBI). This analysis revealed 68.2% sequence identity, suggesting that recognition of the algal BiP by anti-human-BiP antibodies might be possible. As shown in Fig. 2*C*, BiP was readily detectable at significantly up-regulated levels in transgenic *P. purpureum* cells, indicating elevated ER stress upon sE2$^{\Delta HVR1}$ expression. This result suggests that, similar to green algae, *P. purpureum* cells possess the molecular machinery to detect ER stress and are able to respond to it by increasing the ER folding capacity.

Successful production of the His-tagged antigen in *P. purpureum* was confirmed by immunoblotting with anti-His antibodies (*SI Appendix*, Fig. S2*A*), and the strongest expressing line was used for cultivation in a PBR to obtain sufficient antigen amounts for purification. Protein samples were taken daily during the cultivation period and subjected to immunoblot analysis (Fig. 2*E*). The flask-grown cells used to inoculate the PBR (Preculture in Fig. 2*E*) showed antigen accumulation to levels twice as high as the PBR-grown cells. In general, sE2$^{\Delta HVR1}$ accumulation was stable over the time of cultivation, with only a minor decrease observed in the exponential phase.

Quantification of the PBR-derived antigen (sE2$^{\Delta HVR1}$ 2A_a PBR) was performed side-by-side with the strains expressing the other antigen variants grown in flask cultures (Fig. 2*F*). Quantification was done with the same freeze-dried biomass that was later used in the mice feeding experiments. The concentration of the antigen was 0.21% of TP for the PBR-grown sE2$^{\Delta HVR1}$-3xHA strain, with a total antigen concentration of 0.89 μg/mg dry algal biomass (*SI Appendix*, Fig. S2*B*). In our experiments, the final biomass (excluding the exopolysaccharides that were washed off during preparation) was 1.1 g/L for the sE$^{\Delta HVR1}$-3xHA-expressing strain. Considering the cellular antigen accumulation levels of 0.89 mg/g dry weight, this biomass production is equivalent to an approximate antigen yield of 1 mg/L on day 8. Lower total protein content was

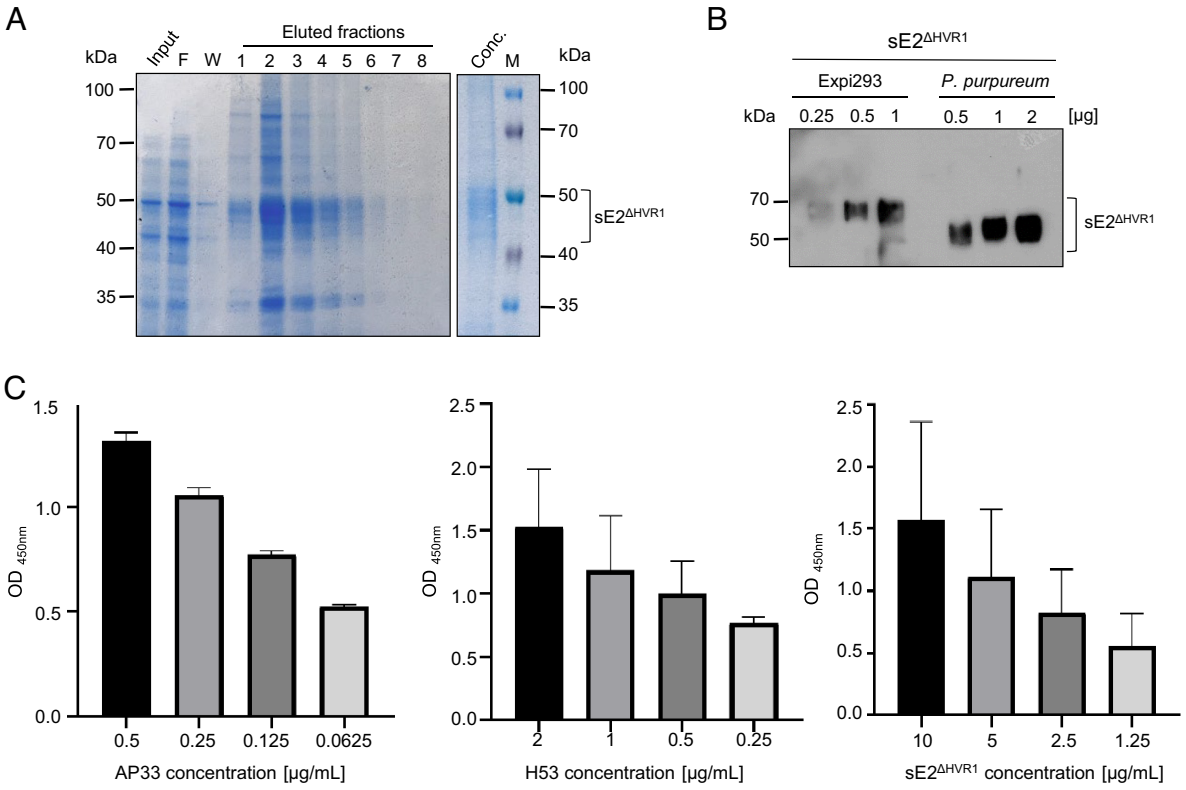

Fig. 3. Purification and characterization of sE2$^{\Delta HVR1}$ expressed in *P. purpureum*. (*A*) *P. purpureum* lysates (Input) were subjected to Ni-NTA chromatography. Binding was done by reloading the column flow-through three times until it was clear of the sE2$^{\Delta HVR1}$ antigen (F). The column was then washed with binding buffer (W). Eluted fractions (1 mL each) were collected and 30 µL from each fraction were separated by SDS-PAGE (10% gel), and subsequently visualized by Coomassie staining (*Left*). The combined PBS-exchanged fractions were concentrated by ultrafiltration through a 30 kDa cut-off Amicon column to a final volume of 1 mL, and a 10 µL sample (Conc.) was separated by SDS-PAGE (10% gel) followed by Coomassie staining (*Right*). M: molecular mass marker. (*B*) Determination of the total amount of purified antigen by immunoblotting using known amounts of Expi293-derived sE2$^{\Delta HVR1}$ as standard. (*C*) Binding of *P. purpureum*–purified sE2$^{\Delta HVR1}$ to anti-E2 antibodies was determined by antigen coating of ELISA plates (200 ng/well) and incubation with serial dilutions of AP33 (*Left*) and H53 (*Middle*) monoclonal antibodies. HRP-labeled rabbit anti-mouse antibodies were used for detection. For receptor binding (*Right*), wells were coated with sE2$^{\Delta HVR1}$ at the indicated concentrations, followed by incubation with 2 µg/mL CD81-LEL-Fc. HRP-labeled goat anti-human-Fc antibodies were used for detection. Mean OD_{450} values from two independent experiments performed in triplicate are presented.

seen for the sE2$^{\Delta HVR1}$-6xHis-expressing strain grown in the PBR, which showed approximately half of the total protein content of the dry biomass compared to the sE2$^{\Delta HVR1}$-3xHA-expressing strain. Variable total protein contents have been described for *P. purpureum* in the literature, with values ranging from 10 to 56% of the dry weight, depending on culture conditions and polysaccharide accumulation (50, 51). Quantification of the sE2$^{\Delta HVR1}$-6xHis antigen was performed after Ni-NTA affinity purification, and gave an approximate yield of 0.5 µg antigen/mg dry weight or 0.25% of TP, which is comparable to the yields of the 3xHA-tagged antigen.

sE2$^{\Delta HVR1}$ Purified from *P. purpureum* Binds Conformation-Dependent Anti-E2 Antibodies and the HCV Receptor CD81. Lysates of sE2$^{\Delta HVR1}$-6xHis-expressing *P. purpureum* were subjected to Ni-NTA affinity chromatography, and antigen-positive fractions were concentrated by ultrafiltration to remove low-molecular-weight contaminants (Fig. 3*A*). The identity of the purified protein was confirmed by immunoblot analysis with anti-His antibodies (*SI Appendix*, Fig. S4). The amount of purified antigen was estimated by comparison with known amounts of pure protein produced in Expi293 cells (Fig. 3*B*). The higher molecular mass of the mammalian cell–derived antigen observed in immunoblots is due to advanced processing and acquisition of complex N-glycans by the secreted protein as compared to the intracellular protein in *P. purpureum.* The antigenicity of *P. purpureum*–derived sE2$^{\Delta HVR1}$ was further tested with monoclonal antibodies specific for linear (AP33) and conformational (H53) epitopes displayed by the native E2 protein (44). Strong recognition of the sE2$^{\Delta HVR1}$ antigen by these antibodies suggests that *P. purpureum* provides the appropriate folding milieu for a complex viral protein to acquire its proper conformation (Fig. 3*C*). This interpretation is further supported by efficient binding of the HCV antigen to the human CD81 receptor, as revealed by ELISA (Fig. 3*C*).

Oral Administration of sE2$^{\Delta HVR1}$-Expressing *P. purpureum* Boosts the Anti-HCV Humoral Immune Response Primed by Injection with the Mammalian Cell–Derived Antigen. We have previously shown that immunization performed by oral administration of lettuce expressing the HCV E1E2 heterodimer, in the absence of adjuvants, resulted in a weak and immature, IgM-based systemic immune response. However, lettuce feeding was able to boost a systemic anti-HCV response primed by injection with E1E2 purified from mammalian cells, characterized by the presence of IgG antibodies, albeit at modest levels (34). To determine the immunogenicity profile of the sE2$^{\Delta HVR1}$ produced in *P. purpureum*, we explored two immunization strategies.

The first approach addressed the capacity of orally administered transgenic algae expressing the 3xHA-tagged sE2$^{\Delta HVR1}$ antigen to support an anti-HCV immune response triggered by injection with pure antigen. Two control groups of five Balb/c mice were three times administered either AddaVax (Adjuvant) or wild-type *P. purpureum*, by intramuscular injection and feeding, respectively.

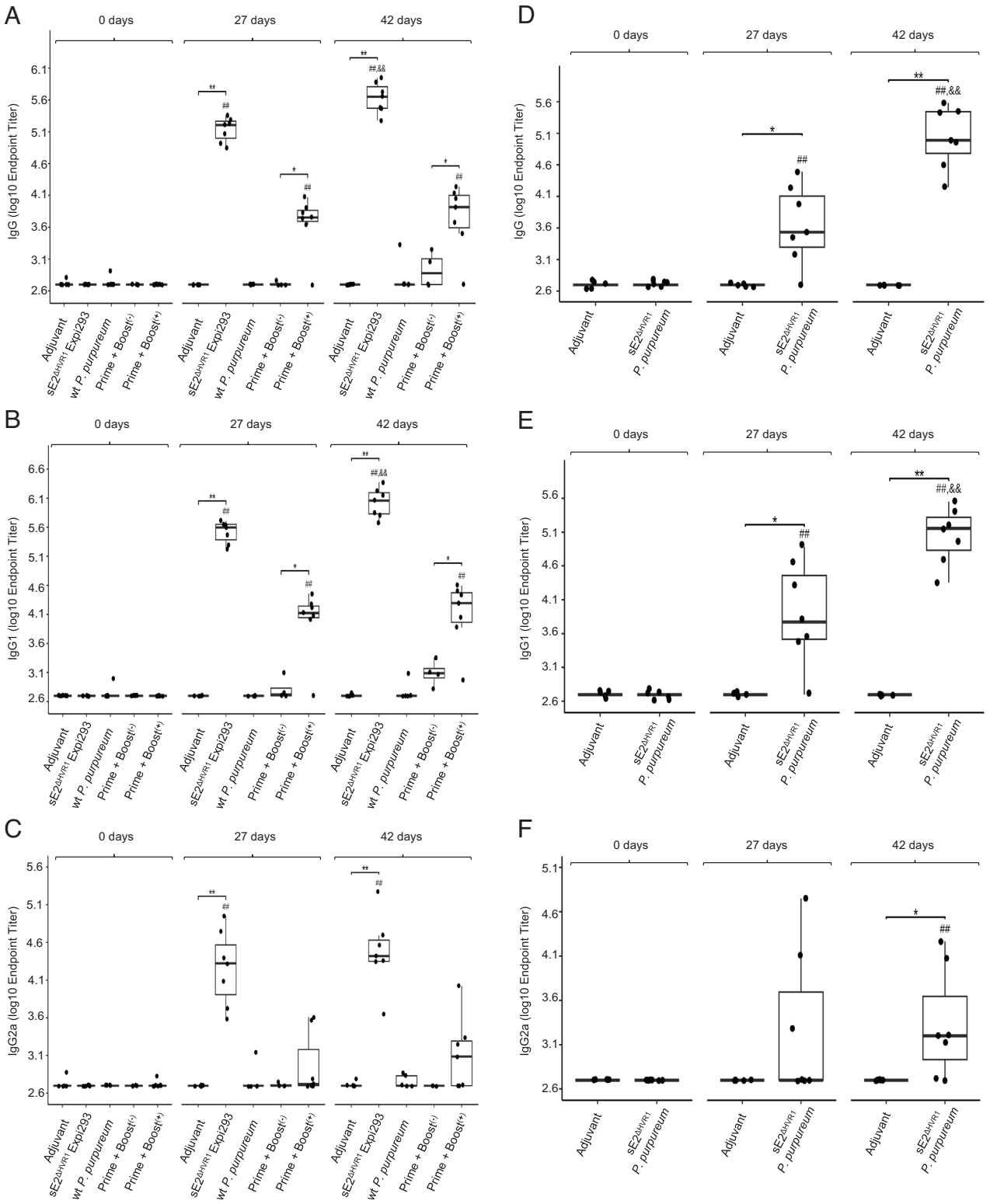

Fig. 4. Characterization of the humoral immune response triggered by oral administration of sE2$^{\Delta HVR1}$–expressing *P. purpureum*, and parenteral immunization with purified sE2$^{\Delta HVR1}$. (*A–C*) Two control groups of 5 Balb/c mice were administered AddaVax (Adjuvant) or 15 mg of wild-type *P. purpureum* three times by intramuscular injection and feeding, respectively. Two groups of seven mice each were first primed by intramuscular injection with 25 μg of Expi293-purified sE2$^{\Delta HVR1}$ followed by two oral administrations of 15 mg of wild type (Prime + Boost$^{(-)}$) or sE2$^{\Delta HVR1}$ *P. purpureum* biomass (Prime + Boost$^{(+)}$). A third group of seven mice was primed and boosted two times by intramuscular injections with 25 μg per dose of the mammalian cell antigen (sE2$^{\Delta HVR1}$ Expi293) in the presence of adjuvant. All immunizations were performed at 14-d intervals. End point titers of IgG (*A*), IgG1 (*B*), and IgG2a (*C*) in mice sera collected at 0, 27, and 42 d postimmunization were calculated based on a 4-parameter logistic regression curve fitted to a pool of immune sera, as the reciprocal sample dilution that would result in three times baseline + SE as derived from the internal standard curve by multiplication. (*D–F*) Groups of four or seven mice were immunized three times, at 14-d intervals, by intramuscular injection with either AddaVax (Adjuvant) or 10 μg/dose of *P. purpureum*–purified sE2$^{\Delta HVR1}$ (sE2$^{\Delta HVR1}$ *P. purpureum*) in the presence of adjuvant. End point titers of IgG (*D*), IgG1 (*E*), and IgG2a (*F*) in sera collected at 0, 27, and 42 d postimmunization were calculated as described above. Statistical analysis was performed using the Wilcoxon rank-sum test. Comparisons between groups at the same time point (*$P < 0.05$; **$P < 0.01$), at days 27 and 42 compared to day 0 (#$P < 0.05$; ##$P < 0.01$), and at day 42 compared to day 27 (&&$P < 0.01$) are shown.

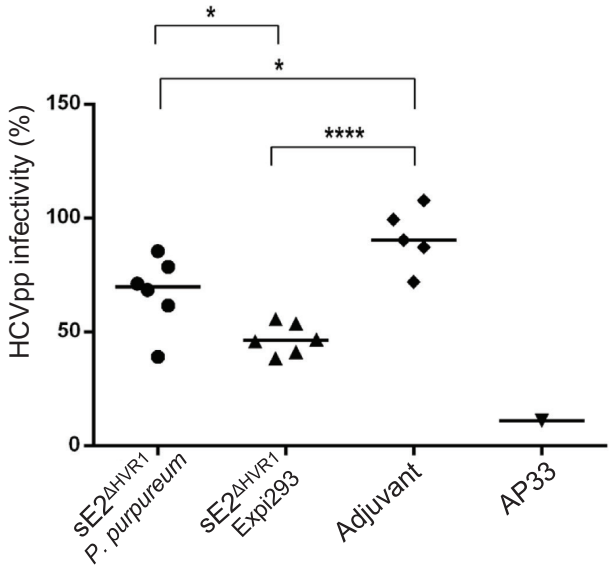

Fig. 5. Neutralization of HCVpp infection by immune sera. Huh7 cells were infected with pseudo-particles (pp) containing a luciferase gene and the HCV-E1E2 envelope (genotype 1a) produced in HEK293T cells. HCVpp infections were performed in the presence of sera from individual mice immunized by intramuscular injections with adjuvant or sE2$^{\Delta HVR1}$ produced in *P. purpureum* (sE2$^{\Delta HVR1}$ *P. purpureum*) or Expi293, as control (dilution 1:50). Anti-HCV-E2 AP33 neutralizing antibodies (10 μg/mL) were used as positive control for specific inhibition of HCVpp infection. The luciferase activity in each sample is represented as percentage of HCVpp infectivity in the presence of individual sera normalized to infected cells in the absence of serum. Shown are mean percentages of two independent experiments performed in triplicate and duplicate, respectively. Black bars indicate the means of the shown values for each condition. Statistical analysis was performed by using the Kruskal–Wallis test (*P < 0.05; ****P < 0.0001).

Two groups of seven mice each were first primed by intramuscular injection with mammalian cell–derived sE2$^{\Delta HVR1}$ purified from Expi293 cell culture medium followed by oral boosting with wild type (Prime + Boost$^{(-)}$) or sE2$^{\Delta HVR1}$ *P. purpureum* biomass (Prime + Boost$^{(+)}$). A third group of seven mice vaccinated exclusively by intramuscular injection with the mammalian sE2$^{\Delta HVR1}$ (Expi293) was also included in the study, as a positive control and indicator of the highest immunological response obtainable in this experimental setting. The presence of total anti-HCV IgG and IgG subclasses in mice sera was monitored before immunization (day 0, preimmune sera) and on days 27 and 42, after the second and third antigen administration, respectively (Fig. 4 *A*–*C*). As expected (34), the parenteral immunization with the sE2$^{\Delta HVR1}$ Expi293 triggered the strongest immune response, with high anti-HCV antibody titers being already evidenced after the first boost, at day 27 (Fig. 4*A*). Interestingly, a significant immune response was also observed in the animal group fed with sE2$^{\Delta HVR1}$, but not with wild-type *P. purpureum*, after priming by injection (Fig. 4*A*). The low anti-HCV titers detected at later time points after oral boosting with wild-type algae is likely the consequence of a slowly maturing, inefficient immune response triggered by the initial injection. This interpretation is strongly supported by the absence of specific anti-HCV antibodies in the control animal group immunized exclusively by feeding with wild-type *P. purpureum*. Recent studies have indicated that the efficiency of the humoral immune response in HCV-infected patients depends on the IgG subclasses induced by natural infection, with high IgG1 and IgG3 titers being detected in individuals who clear the infection (52). An IgG1 subclass-dominant immune response was observed in the groups of mice vaccinated by injection only or by injection followed by feeding (Fig. 4*B*), with a magnitude reflecting the total IgG pattern of the samples (Fig. 4*A*). Notably, significant amounts of IgG2a (Fig. 4*C*) were also detected in these mice, albeit at lower titers than IgG1. Although these antibodies appear to play a minor role in HCV neutralization (52), their presence in mice sera is suggestive of activation of the Th1-based arm of the cellular immune response, associated with a more favorable disease outcome and a sustained virological response after treatment (53, 54).

Fecal levels of IgA, a hallmark of mucosal immunity activation, were also investigated in samples from mice receiving mixed administration. Despite clear activation of a systemic anti-HCV response by this immunization regime (Fig. 4 *A*–*C*), IgA levels remained undetectable at all time points. This may suggest a feeble and transient IgA activation by the E2 antigen in the absence of mucosal adjuvants, as observed in our previous study performed in lettuce (34), or an incomplete absorption of the viral antigen in the gut due to ineffective processing of *P. purpureum* biomass by gastrointestinal enzymes (55).

Parenteral Administration of *P. purpureum*–Derived sE2$^{\Delta HVR1}$ Induces a HCV-Neutralizing Humoral Immune Response in Mice. Having established the immunogenicity of the HCV antigen produced in red algae, we next aimed to optimize this immune response and investigate its potential to prevent HCV infection of host cells in vitro. Therefore, in a second immunization strategy, a systemic administration of the viral antigen purified from transgenic *P. purpureum* cells was investigated. As shown in Fig. 4*D*, a significant HCV-specific systemic immune response was detected in mice following three injections with *P. purpureum*–purified sE2$^{\Delta HVR1}$, but not with adjuvant. The red alga–derived antigen triggered a similar pattern of IgG subclasses as did the mammalian cell–derived counterpart, with a clear shift toward production of IgG1 antibodies (Fig. 4*E*) and a weaker, more heterogeneous, IgG2a response (Fig. 4*F*).

Mice sera were further tested for the presence of neutralizing antibodies against the homologous HCV isolate by using a luciferase-based HCVpp neutralization assay (35). Sera from animals parenterally immunized with Expi293-purified sE2$^{\Delta HVR1}$ were also included in the study, as positive controls for infection neutralization, due to their high IgG titers (Fig. 4*A*). These sera displayed the most potent HCV infection neutralization among the vaccinated mice groups, as anticipated, due to the high amount of antigen used both in prime and boost immunizations (Fig. 5). Remarkably, despite lower overall IgG levels, sera from mice receiving the *P. purpureum* antigen also showed inhibition of HCVpp infection, when compared with the adjuvant group, although the animal response was somewhat more heterogeneous (Fig. 5). It is important to note that the efficiency of HCV neutralization cannot be directly compared between the animal groups receiving mammalian or algal antigens, as immunizations were performed in independent experiments, with significantly different amounts of antigen. The specificity of the HCVpp neutralization assay was further confirmed by the strong inhibitory activity of anti-E2 AP33 monoclonal antibodies, as demonstrated previously (56).

Discussion

In this work, we have investigated the capacity of the red microalga *P. purpureum* to express complex viral proteins that can be used as subunit vaccines against HCV. At present, most biopharmaceuticals are expressed in mammalian cell cultures, due to the requirement for human glycosylation patterns and other (eukaryotic) PTMs. Production in mammalian cell cultures is costly due to expensive culture media and complex cultivation systems. Moreover, the

cultures are prone to contamination with human pathogens, making strict quality controls essential (57). If complex biopharmaceuticals could be produced in a photosynthetic system that is capable of conducting complex PTMs and cannot be infected by animal viruses, the costs of recombinant protein production could be strongly reduced. While it is reasonable to assume that the costs of downstream processing from mammalian cell cultures and microalgal cultures are similar, the costs of biomass production from photosynthetic organisms such as plants and algae will be much lower. It has been calculated that plant-based production platforms can cut the production costs to 0.1% of those of mammalian cell cultures (58), and recent analyses also suggest lower total costs per gram of bioactive compound (59), although large-scale comparative studies are still lacking. Microalgal biomass production will be somewhat more costly than the production of plant biomass (especially when done under sterile conditions and with light supplementation), but will be much cheaper than animal cell cultures, due to the inexpensive culture media for algal growth, the faster growth to high cell densities, and the absence of a contamination risk with human pathogens.

To test the suitability of *P. purpureum* as expression host for proteinaceous biopharmaceuticals, we expressed variants of the $E2^{\Delta HVR1}$ antigen that were targeted to different cellular destinations. The protein was targeted for secretion ($sE2^{\Delta HVR1}$), expressed as an ER-resident protein ($E2^{\Delta HVR1\text{-}HDEL}$), or allowed to accumulate in the cytosol ($^{*}E2^{\Delta HVR1}$). The protein variants could be expressed to amounts between 0.2 and 0.5% of TP, which on average, was four times higher than the expression levels of the same antigens produced in *C. reinhardtii.* Cultivation in a PBR enabled the production of large amounts of biomass, with antigen accumulation reaching 0.5 mg to 0.89 mg/g dry weight and a final yield of approximately 1 mg/L for the $sE2^{\Delta HVR1}$-3xHA antigen. This value can likely be further improved by optimizing cultivation conditions and exploring alternative PBR systems, including wave bag reactors, which may result in higher biomass yields. This future optimization potential notwithstanding, when comparing our current protein yields in *P. purpureum* with those of other glycosylated viral antigens produced in *C. reinhardtii* such as the SARS-CoV-2 spike protein [with reported yields of 31 μg/g fresh weight for the receptor-binding domain (60), and 11.2 μg/L culture for the full protein (61)], the red alga clearly shows superior performance.

Most of the subunit vaccines tested so far for expression in algae were expressed in *C. reinhardtii,* either in the chloroplast (often giving higher protein accumulation than nuclear expression, but with the downside of lack of glycosylation and no possibility to trigger protein secretion into the medium) or from the nuclear genome (allowing secretion and glycosylation, but often suffering from low expression levels, thus precluding comprehensive analysis of their immunogenic properties). Reported chloroplast expression levels range from up to 3% of the total soluble protein (TSP) in the case of the foot and mouth disease virus VP1 protein fused to the cholera toxin B subunit (62) to 0.01% of TSP for the major birch pollen allergen Bet v1 (63). Nuclear transgenes were reported to be expressed to significantly lower levels, ranging from 0.05 to 0.4% of TSP (13, 64, 65). It should be noted that quantification in all of these studies was based on total soluble protein rather than total cellular protein (used as basis for quantification in this work). The soluble proteins account for approximately half of the total protein in *P. purpureum* (18), and therefore, the values reported here should be doubled (thus amounting to approximately 1% of TSP) for proper comparison to the previously reported values. The expression levels achieved with the HCV antigen variants tested here place *P. purpureum* at the top of microalgal nuclear expression systems. Also, the HCV E2 antigen previously produced in *Lactuca sativa* (34) and *Nicotiana benthamiana* (35) reached expression levels of up to 0.1 ng/mg fresh weight and 20 ng/mg fresh weight, respectively, which is far lower than the levels obtained in *P. purpureum*.

We have also shown that *P. purpureum* can faithfully process substantial amounts of correctly folded, N-glycosylated HCV antigen in the ER. As the $sE2^{\Delta HVR1}$ antigen targeted for secretion travels beyond the ER into the Golgi apparatus, the conserved N-glycan core can be further modified in an organism-specific manner, with potential implications for immunogenicity.

Very little was previously known about protein glycosylation in *P. purpureum*. The only available information came from a bioinformatic analysis of enzymes involved in glycosylation and the mass spectrometry-based characterization of an endogenous secreted glycoprotein (40, 66). The mature N-glycan moiety attached to the endogenous protein was determined to be $Man_{8-9}Xyl_{1-2}Me_3GlcNAc_2$ (66). Our mass spectrometric analyses of the affinity-purified *P. purpureum* $sE2^{\Delta HVR1}$ antigen confirmed the presence of similar high-mannose N-linked sugar chains as in mammalian cells. The differences to the previously published glycan structure in *P. purpureum* are likely explained by the nature of the analyzed sample. In our work, the antigen was purified from cells and represents a mixture of glycoforms that result from protein trafficking along the secretory pathway. As likely only the major forms were captured by the mass spectrometric analysis, the presence of alga-specific, late N-glycan maturation events cannot be entirely excluded. Nevertheless, together with the high protein expression level attained, the presence of similar high-mannose N-linked sugar chains as in mammalian cells bodes well for the future use of the red alga as an expression host in molecular farming.

We provide here evidence of the in vivo immunogenicity of an N-glycosylated vaccine candidate expressed from the red algal nuclear genome. Parenteral administration of the *P. purpureum*–derived $sE2^{\Delta HVR1}$ antigen triggered an early and robust humoral immune response. Both the dynamics of this activation and the pattern of the IgG subclasses were similar to those induced by the mammalian cell-expressed counterpart. Remarkably, despite the relatively modest amounts of the algal cell-expressed antigen per dose and the administration of fewer doses in our immunization schedule, compared to other reports (45), the triggered antibodies inhibited HCVpp infection in vitro. The activation of the humoral immune response and the HCV neutralization capacity can likely be further improved by optimizing the immunization parameters. They also should be validated in more physiological HCV infection systems, and ultimately be tested in human patients.

The immunogenic properties of the *P. purpureum*–expressed HCV antigen are supported by the potency of orally administered whole transgenic biomass, to boost the immune response primed by the parenteral route. Interestingly, this combined approach resulted in a significant IgG-based systemic immune response in vaccinated mice, while IgA levels were undetectably low. This result is not unexpected, as mucosal immunity usually requires stimulation by the addition of specific adjuvants such as the well-studied cholera, diphtheria, and heat-labile toxins, or their less toxic derivatives (67). An IgA response may offer extended protection against pathogens that use mucosal surfaces as entry sites. However, in the case of blood-borne viruses such as HCV, a strong systemic immune response is required to neutralize the infection, while a role for mucosal immunity remains obscure (68). Nevertheless, vaccination strategies targeting both mucosal and systemic immune responses can be addressed in future studies by optimizing adjuvant formulations or by fusing antigen candidates with specific

protein subunits and peptides that facilitate mucosal delivery and uptake.

Materials and Methods

Cultivation and Transformation of Microalgae. Cultivation of *P. purpureum* strain SAG 1380-1d and *C. reinhardtii* strain UVM11 was performed as described previously (69, 70; see *SI Appendix, Methods*). Algal growth in photobioreactors is described in *SI Appendix, Methods*. Transformation vectors for *P. purpureum* were constructed based on plasmid pZL22 (17), and vectors for *C. reinhardtii* were constructed based on pRMB19 (65; for details, see *SI Appendix, Methods* and Table S2 and Dataset S1). Nuclear transformation of *P. purpureum* was performed using the biolistic method (18), transformation of *C. reinhardtii* UVM11 was performed using the glass bead method (*SI Appendix, Methods*).

Protein Isolation and Analysis. Protein extraction and precipitation from culture media were done using standard protocols (*SI Appendix, Methods*). Extraction and purification of HCV-E2$^{\Delta HVR1}$-6xHis from *P. purpureum*, glycosidase (Endo H and PNGase F) treatments, immunoblot assays, mass-spectrometric analysis, and antigen-binding assays are described in *SI Appendix, Methods*.

Culture and Transfection of Mammalian Cell Lines. HEK293T and Huh7 cell lines were cultured in Dulbecco's Modified Medium. Transfection and HCVpp production were conducted according to standard procedures (*SI Appendix, Methods*). Expression and purification of HCV-E2$^{\Delta HVR1}$ and the antibodies used for protein detection are described in *SI Appendix, Methods*.

Animals, Immunization, and Analysis of Immune Responses. BALB/c female mice were used for parenteral and oral immunization experiments, as described in *SI Appendix, Methods*. For quantification of the humoral immune response, HCV-specific IgG, IgG1, IgG2a subclasses, and IgA were detected by ELISA, and neutralization of HCV-E1E2 pseudoparticle (pp) infection was analyzed as described previously (35; *SI Appendix, Methods*).

Data, Materials, and Software Availability. All study data are included in the article and/or supporting information. The mass spectrometry-based proteomic data (included in Fig. 1) have been deposited to the ProteomeXchange Consortium via the PRIDE (https://www.ebi.ac.uk/pride/) partner repository with the dataset identifier PXD052401 (71).

ACKNOWLEDGMENTS. This research was supported by EEA Grants 2014–2021, SmartVac project no. 1SEE/2019, the Max Planck Society, and the Norwegian Institute of Bioeconomy Research (NIBIO; project ID 51289). We are grateful to Dr. Jihong Liu Clarke (NIBIO, Ås, Norway) for her invaluable contributions to the initiation of this project and for helpful discussions. L.-M.C. was supported by a PhD fellowship from the Romanian Academy. M.H. was supported by the Deutsche Forschungsgemeinschaft (DFG HI 739/12-4).

Author affiliations: [a]Max-Planck-Institut für Molekulare Pflanzenphysiologie, Department of Organelle Biology, Biotechnology and Molecular Ecophysiology, D-14476 Potsdam-Golm, Germany; [b]Institute of Biochemistry of the Romanian Academy, Department of Viral Glycoproteins, 060031 Bucharest, Romania; [c]"Cantacuzino" Medico-Military National Research Institute, 050096 Bucharest, Romania; [d]Institute of Plant Biology and Biotechnology, University of Münster, D-48143 Münster, Germany; [e]Institute of Plant Science and Resources, Okayama University, Kurashiki 710-0046, Japan; and [f]NIBIO, Norwegian Institute of Bioeconomy Research, NO-1431 Ås, Norway

Author contributions: A.H., L.-M.C., M.H., J.N., C.-I.P., C.S., N.B.-N., and R.B. designed research; A.H., L.-M.C., I.C., I.I., C.T., V.T., A.C., A.O., and L.H. performed research; A.H., L.-M.C., I.C., I.I., C.T., V.T., A.C., A.O., L.H., M.H., J.N., C.-I.P., C.S., N.B.-N., and R.B. analyzed data; and A.H., L.-M.C., C.-I.P., C.S., N.B.-N., and R.B. wrote the paper.

1. M. J. Barbosa, M. Janssen, C. Südfeld, S. D'Adamo, R. H. Wijffels, Hypes, hopes, and the way forward for microalgal biotechnology. *Trends Biotechnol.* **41**, 452–471 (2023).
2. N. Yan, C. Fan, Y. Chen, Z. Hu, The potential for microalgae as bioreactors to produce pharmaceuticals. *Int. J. Mol. Sci.* **17**, 962 (2016).
3. A. Banerjee, V. Ward, Production of recombinant and therapeutic proteins in microalgae. *Curr. Opin. Biotechnol.* **78**, 102784 (2022).
4. J. Neupert, D. Karcher, R. Bock, Generation of *Chlamydomonas* strains that efficiently express nuclear transgenes. *Plant J.* **57**, 1140–1150 (2009).
5. S. E. Shin *et al.*, CRISPR/Cas9-induced knockout and knock-in mutations in *Chlamydomonas reinhardtii*. *Sci. Rep.* **6**, 1–15 (2016).
6. P. Crozet *et al.*, Birth of a photosynthetic chassis: A MoClo toolkit enabling synthetic biology in the microalga *Chlamydomonas reinhardtii*. *ACS Synth. Biol.* **7**, 2074–2086 (2018).
7. J. Neupert *et al.*, An epigenetic gene silencing pathway selectively acting on transgenic DNA in the green alga *Chlamydomonas*. *Nat. Commun.* **11**, 6269 (2020).
8. A. C. V. Bayne *et al.*, Vaccination against influenza with recombinant hemagglutinin expressed by *Schizochytrium* sp. confers protective immunity. *PLoS One* **8**, e61790 (2013).
9. D. Geng, Y. Wang, P. Wang, W. Li, Y. Sun, Stable expression of hepatitis B surface antigen gene in Dunaliella salina (Chlorophyta). *J. Appl. Phycol.* **15**, 451–456 (2003).
10. S. P. Mayfield, S. E. Franklin, R. A. Lerner, Expression and assembly of a fully active antibody in algae. *Proc. Natl. Acad. Sci. U.S.A.* **100**, 438–442 (2003).
11. E. M. Ramos-Martinez, L. Fimognari, Y. Sakuragi, High-yield secretion of recombinant proteins from the microalga *Chlamydomonas reinhardtii*. *Plant Biotechnol. J.* **15**, 1214 (2017).
12. B. A. Rasala *et al.*, Production of therapeutic proteins in algae, analysis of expression of seven human proteins in the chloroplast of *Chlamydomonas reinhardtii*. *Plant Biotechnol. J.* **8**, 719–733 (2010).
13. R. E. Soria-Guerra *et al.*, Expression of an HBcAg-based antigen carrying angiotensin II in *Chlamydomonas reinhardtii* as a candidate hypertension vaccine. *Plant Cell. Tissue Organ Cult.* **116**, 133–139 (2014).
14. Y. He *et al.*, *Chlorella* sp. transgenic with Scy-hepc enhancing the survival of Sparus macrocephalus and hybrid grouper challenged with *Aeromonas hydrophila*. *Fish Shellfish Immunol.* **73**, 22–29 (2018).
15. M. Jarquín-Cordero *et al.*, Towards a biotechnological platform for the production of human pro-angiogenic growth factors in the green alga *Chlamydomonas reinhardtii*. *Appl. Microbiol. Biotechnol.* **104**, 725–739 (2020).
16. J. Hernández-Ramírez, A. Wong-Arce, O. González-Ortega, S. Rosales-Mendoza, Expression in algae of a chimeric protein carrying several epitopes from tumor associated antigens. *Int. J. Biol. Macromol.* **147**, 46–52 (2020).
17. Z. Li, R. Bock, Replication of bacterial plasmids in the nucleus of the red alga *Porphyridium purpureum*. *Nat. Commun.* **9**, 3451 (2018).
18. A. Hammel, J. Neupert, R. Bock, Optimized transgene expression in the red alga *Porphyridium purpureum* and efficient recombinant protein secretion into the culture medium. *Plant Mol. Biol.* **114**, 18 (2024).
19. World Health Organization, Hepatitis C. Fact Sheet Number 164. https://www.who.int/en/news-room/fact-sheets/detail/hepatitis-c. Accessed 4 November 2023.
20. M. P. Manns *et al.*, Hepatitis C virus infection. *Nat. Rev. Dis. Prim.* **3**, 1–19 (2017).
21. R. Bartenschlager *et al.*, Critical challenges and emerging opportunities in hepatitis C virus research in an era of potent antiviral therapy: Considerations for scientists and funding agencies. *Virus Res.* **248**, 53–62 (2018).
22. J. H. Salas *et al.*, An antigenically diverse, representative panel of envelope glycoproteins for hepatitis c virus vaccine development. *Gastroenterology* **162**, 562–574 (2022).
23. N. Tzarum, I. A. Wilson, M. Law, The neutralizing face of hepatitis C virus E2 envelope glycoprotein. *Front. Immunol.* **9**, 1315 (2018).
24. M. Lavie, A. Goffard, J. Dubuisson, Assembly of a functional HCV glycoprotein heterodimer. *Curr. Issues Mol. Biol.* **9**, 71–86 (2007).
25. A. Kumar *et al.*, Structural insights into hepatitis C virus receptor binding and entry. *Nature* **598**, 521–525 (2021).
26. J. M. Pfaff-Kilgore *et al.*, Sites of vulnerability in HCV E1E2 identified by comprehensive functional screening. *Cell Rep.* **39**, 110859 (2022).
27. P. Colombatto *et al.*, HCV E1E2-MF59 vaccine in chronic hepatitis C patients treated with PEG-IFNα2a and Ribavirin: A randomized controlled trial. *J. Viral Hepat.* **21**, 458 (2014).
28. J. L. M. Law *et al.*, A hepatitis C virus (HCV) vaccine comprising envelope glycoproteins gpE1/gpE2 derived from a single isolate elicits broad cross-genotype neutralizing antibodies in humans. *PLoS One* **8**, e59776 (2013).
29. A. G. Khan *et al.*, Structure of the core ectodomain of the hepatitis C virus envelope glycoprotein 2. *Nature* **509**, 381–384 (2014).
30. L. Kong *et al.*, Hepatitis C virus E2 envelope glycoprotein core structure. *Science (80-.)* **342**, 1090–1094 (2013).
31. T. Krey *et al.*, The disulfide bonds in glycoprotein E2 of hepatitis C virus reveal the tertiary organization of the molecule. *PLoS Pathog.* **6**, e1000762 (2010).
32. D. Li *et al.*, Altered glycosylation patterns increase immunogenicity of a subunit hepatitis C virus vaccine, inducing neutralizing antibodies which confer protection in mice. *J. Virol.* **90**, 10486 (2016).
33. B. G. Pierce *et al.*, Structure-based design of hepatitis C virus E2 glycoprotein improves serum binding and cross-neutralization. *J. Virol.* **94**, e00704-20 (2020).
34. J. L. Clarke *et al.*, Lettuce-produced hepatitis C virus E1E2 heterodimer triggers immune responses in mice and antibody production after oral vaccination. *Plant Biotechnol. J.* **15**, 1611–1621 (2017).
35. M. O. Dobrica *et al.*, Hepatitis C virus E2 envelope glycoprotein produced in *Nicotiana benthamiana* triggers humoral response with virus-neutralizing activity in vaccinated mice. *Plant Biotechnol. J.* **19**, 2027 (2021).
36. P. T. Vietheer *et al.*, The core domain of hepatitis C virus glycoprotein E2 generates potent cross-neutralizing antibodies in guinea pigs. *Hepatology* **65**, 1117–1131 (2017).
37. B. G. Pierce *et al.*, Structure-based design of hepatitis C virus vaccines that elicit neutralizing antibody responses to a conserved epitope. *J. Virol.* **91**, 1032–1049 (2017).
38. T. Khera *et al.*, Functional and immunogenic characterization of diverse HCV glycoprotein E2 variants. *J. Hepatol.* **70**, 593–602 (2019).
39. T. Baier, J. Wichmann, O. Kruse, K. J. Lauersen, Intron-containing algal transgenes mediate efficient recombinant gene expression in the green microalga *Chlamydomonas reinhardtii*. *Nucleic Acids Res.* **46**, 6909–6919 (2018).
40. X. Liu *et al.*, Bioinformatic analysis and genetic engineering approaches for recombinant biopharmaceutical glycoproteins production in microalgae. *Algal Res.* **55**, 102276 (2021).
41. M. Azim, H. Surani, Glycoprotein synthesis and inhibition of glycosylation by tunicamycin in preimplantation mouse embryos: Compaction and trophoblast adhesion. *Cell* **18**, 217–227 (1979).
42. J. Bräutigam, A. J. Scheidig, W. Egge-Jacobsen, Mass spectrometric analysis of hepatitis C viral envelope protein E2 reveals extended microheterogeneity of mucin-type O-linked glycosylation. *Glycobiology* **23**, 453–474 (2013).

43. S. Duvet *et al.*, Hepatitis C virus glycoprotein complex localization in the endoplasmic reticulum involves a determinant for retention and not retrieval. *J. Biol. Chem.* **273**, 32088–32095 (1998).
44. L. Cocquerel, J.-C. Meunier, A. Pillez, C. Wychowski, J. Dubuisson, A retention signal necessary and sufficient for endoplasmic reticulum localization maps to the transmembrane domain of hepatitis C virus glycoprotein E2. *J. Virol.* **72**, 2183–2191 (1998).
45. R. A. Urbanowicz *et al.*, Antigenicity and immunogenicity of differentially glycosylated hepatitis C virus E2 envelope proteins expressed in mammalian and insect cells. *J. Virol.* **93**, e01403-18 (2019).
46. E. Little, M. Ramakrishnan, B. Roy, G. Gazit, A. S. Lee, The glucose-regulated proteins (GRP78 and GRP94): Functions, gene regulation, and applications. *Crit. Rev. Eukaryot. Gene Expr.* **4**, 1–18 (1994).
47. S. H. Howell, Evolution of the unfolded protein response in plants. *Plant. Cell Environ.* **44**, 2625–2635 (2021).
48. M. Schroda, The *Chlamydomonas* genome reveals its secrets: Chaperone genes and the potential roles of their gene products in the chloroplast. *Photosynth. Res.* **82**, 221–240 (2004).
49. S. Díaz-Troya *et al.*, Inhibition of protein synthesis by TOR inactivation revealed a conserved regulatory mechanism of the BiP chaperone in *Chlamydomonas*. *Plant Physiol.* **157**, 730–741 (2011).
50. S. Li, L. Ji, Q. Shi, H. Wu, J. Fan, Advances in the production of bioactive substances from marine unicellular microalgae *Porphyridium* spp. *Bioresour. Technol.* **292**, 122048 (2019).
51. C. Safi, M. Charton, O. Pignolet, P. Y. Pontalier, C. Vaca-Garcia, Evaluation of the protein quality of *Porphyridium cruentum*. *J. Appl. Phycol.* **25**, 497–501 (2013).
52. M. R. Walker *et al.*, Envelope-specific IgG3 and IgG1 responses are associated with clearance of acute hepatitis C virus infection. *Viruses* **12**, 75 (2020).
53. S. Sobue *et al.*, Th1/Th2 cytokine profiles and their relationship to clinical features in patients with chronic hepatitis C virus infection. *J. Gastroenterol.* **36**, 544–551 (2001).
54. J. K. Flynn *et al.*, Maintenance of Th1 hepatitis C virus (HCV)-specific responses in individuals with acute HCV who achieve sustained virological clearance after treatment. *J. Gastroenterol. Hepatol.* **28**, 1770–1781 (2013).
55. L. Machado, G. Carvalho, R. N. Pereira, Effects of innovative processing methods on microalgae cell wall: Prospects towards digestibility of protein-rich biomass. *Biomass* **2**, 80–102 (2022).
56. I. Desombere *et al.*, Monoclonal anti-envelope antibody AP33 protects humanized mice against a patient-derived hepatitis C virus challenge. *Hepatology* **63**, 1120 (2016).
57. F. V. Ritacco, Y. Wu, A. Khetan, Cell culture media for recombinant protein expression in Chinese hamster ovary (CHO) cells: History, key components, and optimization strategies. *Biotechnol. Prog.* **34**, 1407–1426 (2018).
58. R. M. Twyman, E. Stöger, S. Schillberg, P. Christou, R. Fischer, Molecular farming in plants: Host systems and expression technology. *Trends Biotechnol.* **21**, 570–578 (2003).
59. P. Mir-Artigues *et al.*, A simplified techno-economic model for the molecular pharming of antibodies. *Biotechnol. Bioeng.* **116**, 2526–2539 (2019).
60. A. J. Berndt *et al.*, Recombinant production of a functional SARS-CoV-2 spike receptor binding domain in the green algae *Chlamydomonas reinhardtii*. *PLoS One* **16**, e0257089 (2021).
61. A. M. Kiefer, J. Niemeyer, A. Probst, G. Erkel, M. Schroda, Production and secretion of functional SARS-CoV-2 spike protein in *Chlamydomonas reinhardtii*. *Front. Plant Sci.* **13**, 988870 (2022).
62. M. Sun *et al.*, Foot-and-mouth disease virus VP1 protein fused with cholera toxin B subunit expressed in *Chlamydomonas reinhardtii* chloroplast. *Biotechnol. Lett.* **25**, 1087–1092 (2003).
63. S. Hirschl *et al.*, Expression and characterization of functional recombinant bet v 1.0101 in the chloroplast of *Chlamydomonas reinhardtii*. *Int. Arch. Allergy Immunol.* **173**, 44–50 (2017).
64. A. Kumar, V. R. Falcao, R. T. Sayre, Evaluating nuclear transgene expression systems in *Chlamydomonas reinhardtii*. *Algal Res.* **2**, 321–332 (2013).
65. R. Barahimipour, J. Neupert, R. Bock, Efficient expression of nuclear transgenes in the green alga *Chlamydomonas*: Synthesis of an HIV antigen and development of a new selectable marker. *Plant Mol. Biol.* **90**, 403–418 (2016).
66. O. Levy-Ontman *et al.*, Unique N-glycan moieties of the 66-kDa cell wall glycoprotein from the red microalga *Porphyridium* sp. *J. Biol. Chem.* **286**, 21340–21352 (2011).
67. V. A. Correa, A. I. Portilho, E. De Gaspari, Vaccines, adjuvants and key factors for mucosal immune response. *Immunology* **167**, 124–138 (2022).
68. A. Iwasaki, Exploiting mucosal immunity for antiviral vaccines. *Annu. Rev. Immunol.* **34**, 575–608 (2016).
69. S. Kathiresan, R. Sarada, S. Bhattacharya, G. A. Ravishankar, Culture media optimization for growth and phycoerythrin production from *Porphyridium purpureum*. *Biotechnol. Bioeng.* **96**, 456–463 (2007).
70. J. Neupert, N. Shao, Y. Lu, R. Bock, "Genetic transformation of the model green alga *Chlamydomonas reinhardtii*" in *Methods in Molecular Biology*, N. J. Clifton, Ed. (2012), pp. 35–47.
71. A. Hammel *et al.*, The red alga Porphyridium as a host for molecular farming: Efficient production of immunologically active hepatitis C virus glycoprotein. PRIDE Proteomics Identifications Database. https://www.ebi.ac.uk/pride/archive/projects/PXD052401. Deposited 20 May 2024.